

Development of novel robust nanobiocatalyst for detergents formulations and the other applications of alkaline protease

Abdelnasser S. S. Ibrahim^{1,2} · Ahmed M. El-Toni^{3,4} · Ali A. Al-Salamah¹ · Khalid S. Almaary¹ · Mohamed A. El-Tayeb¹ · Yahya B. Elbadawi¹ · Garabed Antranikian⁵

Received: 24 January 2016 / Accepted: 29 January 2016 / Published online: 10 February 2016
© Springer-Verlag Berlin Heidelberg 2016

Abstract Alkaline protease from alkaliphilic *Bacillus* sp. NPST-AK15 was immobilized onto functionalized and non-functionalized rattle-type magnetic core@mesoporous shell silica (RT-MCMSS) nanoparticles by physical adsorption and covalent attachment. However, the covalent attachment approach was superior for NPST-AK15 protease immobilization onto the activated RT-MCMSS-NH₂ nanoparticles and was used for further studies. In comparison to free protease, the immobilized enzyme exhibited a shift in the optimal temperature and pH from 60 to 65 °C and pH 10.5–11.0, respectively. While free protease was completely inactivated after treatment for 1 h at 60 °C, the immobilized enzyme maintained 66.5 % of its initial activity at similar conditions. The immobilized protease showed higher k_{cat} and K_m , than the soluble enzyme by about 1.3-, and 1.2-fold, respectively. In addition, the results revealed significant

improvement of NPST-AK15 protease stability in variety of organic solvents, surfactants, and commercial laundry detergents, upon immobilization onto activated RT-MCMSS-NH₂ nanoparticles. Importantly, the immobilized protease maintained significant catalytic efficiency for ten consecutive reaction cycles, and was separated easily from the reaction mixture using an external magnetic field. To the best of our knowledge this is the first report about protease immobilization onto rattle-type magnetic core@mesoporous shell silica nanoparticles that also defied activity-stability tradeoff. The results clearly suggest that the developed immobilized enzyme system is a promising nanobiocatalyst for various bioprocess applications requiring a protease.

Keywords Nanobiotechnology · Alkaliphiles · Proteases · Enzyme immobilization · Rattle-type magnetic core@mesoporous shell silica nanoparticles

Electronic supplementary material The online version of this article (doi:10.1007/s00449-016-1559-z) contains supplementary material, which is available to authorized users.

✉ Abdelnasser S. S. Ibrahim
ashebl@ksu.edu.sa

¹ Department of Botany and Microbiology, College of Science, King Saud University, Riyadh 11451, Saudi Arabia

² Department of Chemistry of Natural and Microbial Products, National Research Center, El-Buhouth St., Dokki, Cairo 12311, Egypt

³ King Abdullah Institute for Nanotechnology, King Saud University, Riyadh 11451, Saudi Arabia

⁴ Central Metallurgical Research and Development Institute, Helwan 11421, Cairo, Egypt

⁵ Institute of Technical Microbiology, Hamburg University of Technology, 21073 Hamburg, Germany

Abbreviations

APMS	3-Aminopropyltrimethoxysilane
BET	Brunauer–Emmett–Teller
BJH	Barrett–Joyner–Halenda
BTME	1,2-Bis(trimethoxysilyl)ethane
CTAB	Cetyl-trimethylammonium bromide
FT-IR	Fourier transform-infrared
k_{cat}/K_m	Catalytic efficiency
k_{cat}	Enzyme turnover number
K_m	Michaelis–Menten constant
MPS	Mesoporous silica
RT-MCMSS-C ₂ H ₅	Ethan-type magnetic core@mesoporous shell silica
RT-MCMSS-NH ₂	Amino-functionalized rattle-type magnetic core@mesoporous shell silica

RT-MCMSS-non	Non-functionalized rattle-type magnetic core@mesoporous shell silica
SDS	Sodium dodecyl sulfate
TCA	Trichloroacetic acid
TEM	Transmission electron microscopy
TEOS	Tetraethyl orthosilicate
V_{\max}	Maximum enzyme reaction rate

Introduction

Currently there is an increasing application of microbial enzymes replacing chemical catalysts in various biochemical processes, manufacturing chemicals and pharmaceuticals [1]. Proteases constitute one of the most important groups of industrial enzymes, accounting up to 60 % of the total enzyme market with two-thirds of the proteases produced commercially from microbial origin [2–5]. Proteases are a large group of hydrolytic enzymes that catalyze the degradation of the proteins molecules by cleavage of the peptide bonds between the amino acid residues. Alkaline proteases, with high activity and stability in alkaline range, are interesting for several biotechnological applications, particularly for detergent industry [6]. Detergent formulations showed biggest worldwide enzyme consumption, accounting for approximately 30 % of the total world enzyme production [7].

Generally, the activity, stability and reusability of soluble enzymes are of major concerns which limit their industrial applications owing to its impact on the bioprocess cost [1, 8]. Immobilization of soluble enzymes on a variety of water-insoluble supports is one of the most useful approaches to overcome such difficulties. Application of immobilized enzymes in bioprocesses can offer several advantages over the free enzyme such as reusability of the enzyme, enhancement of the biocatalyst stability, better bioprocess control, and simplifying product purification [9, 10]. Recent advance in nanotechnology has provided diverse nanoscaffolds that could potentially support enzymes immobilization technology [11–13].

Nanoscale materials can offer many unique and advantageous physicochemical capabilities for enzyme immobilization, due in part to high surface area/volume ratios that enhance catalysis; effective mass transfer, and high enzyme loading [12, 13]. However, selection of suitable supporting matrix and the immobilization protocols is of significant importance for successful enzyme immobilization process. Among those nanostructured materials, mesoporous silica (MPS) nanoparticles are of special interest for enzyme immobilization technology. MPS provide tunable and uniform pore system, functionalizable surfaces, large

surface areas, and restricted nanospaces for enzymes immobilization, in addition to high biocompatibility and low cytotoxicity [14]. Furthermore, to overcome the difficulty of nanoparticles separation from the bulk solution, mesoporous shell can be coated on magnetic Fe_3O_4 nanocores to form core–shell structure. Magnetic Fe_3O_4 -mesoporous shell silica spheres showed promising results for immobilization of enzyme together with ability for facile separation from bulk solution using magnetic field [10]. Furthermore, creating a cavity between outer mesoporous silica shell and inner silica coated Fe_3O_4 nanocore, formation of rattle structure, could provide more nanospaces for accommodating and immobilizing enzymes [15]. Figure 1 shows scheme for synthesis of rattle-type magnetic core/mesoporous shell silica ($\text{Fe}_3\text{O}_4@m\text{-SiO}_2$) nanoparticles, ethane/amino functionalization and enzyme immobilization.

In the present study, a recently characterized alkaline serine protease from halotolerant alkaliphilic *Bacillus* sp. NPST-AK15 [16] was immobilized onto rattle-type magnetic core/mesoporous shell silica (RT-MCMSS) nanoparticles by physical adsorption and covalent attachment. Subsequently, the properties of immobilized protease were evaluated compared with the free enzyme.

Materials and methods

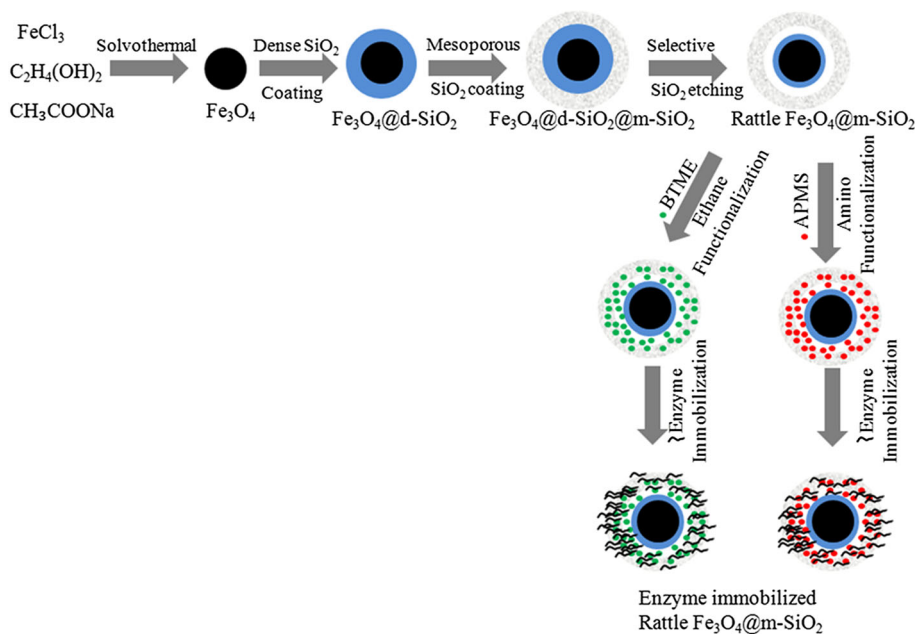
Alkaline protease production and purification

Alkaline serine protease from halotolerant alkaliphilic *Bacillus* sp. NPST-AK15 was recently purified and characterized [16]. For enzyme production, one hundred milliliter of the production medium in 500 mL Erlenmeyer flasks was inoculated with 2 mL of an overnight culture grown at 40 °C and 150 rpm. These cultures were cultivated under the same conditions for approximately 36 h. The production medium contained (pH 10.5): yeast extract (7.5 g/L), fructose (20 g/L), K_2HPO_4 (1.0 g/L), $\text{Mg}_2\text{SO}_4 \cdot 7\text{H}_2\text{O}$ (0.2 g/L), NaCl (50 g/L), and Na_2CO_3 (10 g/L). After the incubation period, the culture was centrifuged to remove cells and insoluble residues; culture supernatant was filtered and used as the enzyme source. Alkaline protease was purified from *Bacillus* sp. NPST-AK15 culture supernatant using combination of ammonium sulfate precipitation and anion exchange column chromatography as described previously [16].

Synthesis of rattle-type magnetic core@mesoporous shell silica nanoparticles

The synthesis of non-functionalized and functionalized rattle-type magnetic core@mesoporous shell silica (RT-

Fig. 1 Scheme for synthesis of rattle-type magnetic core/mesoporous shell silica ($\text{Fe}_3\text{O}_4@m\text{-SiO}_2$) nanoparticles, ethane/amino functionalization and enzyme immobilization



MCMSS) nanoparticles included (1) Synthesis of dense silica coated magnetic Fe_3O_4 nanoparticle; (2) Mesoporous shell formation on the dense silica coated Fe_3O_4 nanoparticles; (3) Rattle-type magnetic core/mesoporous shell silica (RT-MCMSS) formation, and (4) functionalization of the RT-MCMSS nanoparticles (Fig. 1).

Synthesis of silica coated magnetic Fe_3O_4 nanoparticle

Solvothermal reaction was applied for synthesis of magnetic Fe_3O_4 (magnetite) nanoparticles according to Deng et al. [17] with some modification. Briefly, 2.7 g $\text{FeCl}_3 \cdot 6\text{H}_2\text{O}$ was dissolved in 80 mL ethylene glycol, followed by addition of 7.2 g Na-acetate and 2.0 g polyethylene glycol. The mixture was stirred vigorously for 1 h and then sealed in a stainless-steel 100 mL capacity-autoclave (Teflon lined). The autoclave was maintained at 190 °C for 18 h, and the black product was washed several times with ethanol and dried for 6–8 h at 60 °C. To avoid leaching of the iron oxide onto the mother system under acidic conditions, the synthesized magnetic Fe_3O_4 nanoparticles were coated with dense silica layer according to Deng et al. [18]. Typically, 6 mL of the synthesized Fe_3O_4 nanoparticles suspended in ethanol (9.77 mg/mL) was dispersed in mixture of 60 mL ethanol, 5.2 mL dH_2O , and 2.4 mL concentrated ammonia solution. Then, 0.5 mL of tetraethyl orthosilicate (TEOS) was added and the mixture stirred at room temperature for 90 min. The resulted silica coated Fe_3O_4 nanoparticles were separated using an external magnetic field and washed several times with ethanol.

Mesoporous shell formation on dense silica coated Fe_3O_4 nanoparticles

The synthesized silica coated Fe_3O_4 nanoparticles were further coated with mesoporous silica shell to give magnetic core@dense silica@mesoporous shell nanoparticles using previously reported method [19]. Briefly, 0.6 g cetyltrimethylammonium bromide (CTAB) was dissolved in 80 mL of water/ethanol mixture (1:1), and then 1 mL ammonia solution (28 %) was added, to give solution A. In solution B, the synthesized silica coated Fe_3O_4 nanoparticles were dispersed onto 180 mL water/ethanol mixture (2:1) by sonication for 15 min. Thereafter, solution A was added to solution B with stirring for 10 min, followed by dropwise addition of 1.2 mL tetraethyl orthosilicate (TEOS) with stirring for 4 h. The resulted magnetic core@dense silica@mesoporous shell nanoparticles were separated using an external magnetic field and washed several times with ethanol.

Rattle-type magnetic core/mesoporous shell silica (RT-MCMSS) nanoparticles

The middle dense silica layer of the magnetic core@dense silica@mesoporous shell nanoparticles was selectively etched to produce rattle-type magnetic core@mesoporous silica shell (RT-MCMSS) nanoparticles. The etching process takes place onto a Na_2CO_3 solution via a cationic-surfactant-assisted selective etching route [20]. Typically 100 mg of the magnetic core@dense silica@mesoporous shell nanoparticles was dispersed in 15 mL of H_2O under ultrasonic treatment followed by the addition of 55 mg of

Na_2CO_3 and stirred at 50 °C for 8 h. The products were collected using an external magnetic field and washed with deionized water and ethanol several times. For non-functionalized rattle-type magnetic core/mesoporous silica shell (RT-MCMSS-non) nanoparticles, the final powder was dispersed in 60 mL of NH_4NO_3 /ethanol solution (6 g/l) and refluxed at 60 °C for 1 h at room temperature. This extraction process was repeated twice.

Functionalization of RT-MCMSS nanoparticles

Amino- and ethane functionalization of RT-MCMSS nanoparticles was performed using 3-aminopropyltrimethoxysilane (APMS) and 1,2-bis(trimethoxysilyl)ethane (BTME), respectively, through the post-synthesis functionalization approach according to Yang et al. [21]. For RT-MCMSS- NH_2 synthesis, 3.5 mL of APMS was added to suspension of freshly evacuated RT-MCMSS nanoparticles (7 g) in 120 mL toluene. For RT-MCMSS- C_2H_5 , 1 mL of BTME was added to suspensions of freshly evacuated RT-MCMSS (2 g) in 34 mL toluene. The reaction mixtures were heated at 120 °C for 3 h with stirring. The modified solids were separated and washed with a diethyl ether–dichloromethane mixture (1:1).

Characterization of the nanomaterials

Nitrogen sorption isotherms were measured at 77 K with a Quantachrome NOVA 4200 analyzer (USA). Before measurements, the samples were degassed in a vacuum at 200 °C for at least 18 h. The specific surface area was calculated using adsorption data at the relative pressure range from 0.02 to 0.20, utilizing the Brunauer–Emmett–Teller (BET) method. Barrett–Joyner–Halenda (BJH) model was used for deriving the pore volumes and size distributions from the adsorption branches of isotherms and the total pore volumes (V_t) were estimated from the adsorbed amount at a relative pressure P/P_0 of 0.995. The Fourier transform-infrared (FT-IR) spectra were recorded using a Bruker Vertex-80 spectrometer. Transmission electron microscopy (TEM) images were obtained using a JEOL JSM-2100F electron microscope (Japan) operated at 200 kV. The magnetic character for the samples was measured by superconducting quantum interference device (SQUID) magnetometer.

Alkaline protease immobilization

Covalent attachment

For covalent immobilization of the purified NPST-AK15 alkaline protease onto the amino-functionalized rattle-type magnetic core@mesoporous silica shell (RT-MCMSS-

NH_2) nanoparticles, the support was first activated by glutaraldehyde ($\text{OCHCH}_2\text{CH}_2\text{CHO}$) as bifunctional cross linker agent (Fig. 1), followed by the coupling of the enzyme to the activated nanoparticles [10, 22]. Briefly, 100 mg of the RT-MCMSS- NH_2 nanoparticles was suspended in 10 mL of aqueous glutaraldehyde solution (5 %, v/v), and the mixture was incubated with stirring at room temperature for 2 h. Thereafter, the activated support was collected from the solution using an external magnetic field, and washed several times with distilled water to remove the excess glutaraldehyde. Then, the activated support was resuspended in 1 mL glycine buffer (50 mM, pH 8) containing the purified NPST-AK15 protease (12.5 mg) and maintained overnight at 4 °C with gentle shaking. The enzyme-bound nanoparticles were recovered by external magnetic field, and washed twice with the same buffer to remove any unbound protease. The washed solution was collected for protein content and protease activity measurement.

Physical adsorption

Three rattle-type magnetic core@mesoporous silica shell nanoparticles samples were used for NPST-AK15 protease immobilization by physical adsorption including: RT-MCMSS-non; RT-MCMSS- NH_2 , and RT-MCMSS- C_2H_5 (Fig. 1) according to previously reported method [23]. Briefly, 100 mg of various supports was suspended in 1 mL of 50 mM glycine buffer (pH 8) containing the purified NPST-AK15 protease, and maintained overnight with gentle shaking at 4 °C. The enzyme-bound nanoparticles were collected by external magnetic field, and washed twice with glycine buffer to remove the unbound protease. The washed solution was kept for measurement of protein content and protease activity.

Assay of alkaline protease activity

Protease activity of free and immobilized enzyme was measured using casein as a substrate in accordance with previously described method, with some modification [8]. A 0.75 mL of 50 mM glycine buffer (pH 10.0) containing 1 % (w/v) casein was pre-incubated for 5 min at 50 °C. Then, a 0.75-mL aliquot of suitably diluted free NPST-AK15 protease or 0.75-mL glycine buffer containing 50 mg of immobilized enzyme was mixed with the substrate solution and incubated for 20 min at 50 °C. To terminate the reaction, 0.75 mL of 20 % (w/v) trichloroacetic acid (TCA) was added, allowed to stand at room temperature for 15 min and centrifuged at $6000\times g$ for 15 min to remove the precipitate. A controlled reaction was performed in the same manner, except that TCA was added to the substrate prior to the addition enzyme. The acid soluble

materials were estimated using Lowry method using tyrosine as a standard [24]. One unit of protease activity was defined as amount of enzyme required to liberate 1 μg of tyrosine per minute under the experimental conditions. Protein concentration was determined by Lowry method using bovine serum albumin as a standard protein [24]. The loading efficiency (%), immobilization activity and yields were calculated according to Song et al. [25]: loading efficiency = $[(P_i - P_{\text{unb}})/P_i] \times 100$, where P_i and P_{unb} are the initial protein subjected to immobilization, and the unbound protein, respectively. Immobilization yield (%) = $[(A - B)/A] \times 100$, where A is the total activity of the enzyme added in the initial immobilization solution and B is the activity of the unbound protease. Activity yield = $(C/A) \times 100$, where A is the total activity of the enzyme added in the initial immobilization solution, and C is activity of the immobilization protease.

Properties of the immobilized alkaline protease

Effect of temperature

The influence of temperature on the activity of free and immobilized NPST-AK15 protease was investigated by measuring the enzyme activity at different temperatures (30–75 °C) under standard assay conditions. For determination of NPST-AK15 protease thermal stability, the free and immobilized enzymes prepared in 50 mM glycine buffer (pH 8) were incubated at different temperatures (40–60 °C) in a shaking water bath and aliquots were periodically withdrawn at 20 min intervals. The samples were cooled immediately in an ice bath, and the residual activity of the free and immobilized protease was measured and compared with the untreated enzymes.

Effect of pH

The optimum pH for activity of free and immobilized NPST-AK15 protease was determined by measuring the enzyme activity at various pH (pH 5–13), using suitable buffers including: 50 mM sodium acetate (pH 5.0 and 6.0), 50 mM Tris-HCl (pH 7.0 and 8.0), 50 mM glycine-NaOH buffer (9.0–10.5) and 50 mM carbonate-bicarbonate buffer (pH 11.0–13.0). In addition, the pH stability of the free and immobilized protease was investigated by incubating the enzyme samples in buffers at the different pH for 3 h at room temperature (25 °C), and the residual activity of the enzymes was assayed under standard assay conditions.

Effect of salinity

The influence of salinity on activity of free and immobilized protease was determined by measuring the enzyme

activity in the presence of different NaCl concentrations (0–25 %). In addition, the salinity stability of the free and immobilized NPST-AK15 enzyme was investigated by pre-incubating the enzyme for 1 h at different NaCl concentrations ranging from 0.0 to 25.0 %, and the residual activity was measured under standard assay conditions. The activity of the enzyme determined without NaCl was used as a control.

Effect of surfactants, solvents, and commercial detergents

The stability of free and immobilized NPST-AK15 protease was monitored in the presence of some surfactants including Tween 80, Triton X-100, polyethylene-block-poly(ethylene glycol), cetyl-trimethylammonium bromide (CTAB), lauryl glucoside, and sodium dodecyl sulfate (SDS). The free and immobilized enzymes were pre-incubated with the additives at concentrations of 1.0 and 5.0 % at 40 °C for 1 h, and the residual protease activity was measured at standard assay conditions. In addition, the influence of organic solvents on stability of free and immobilized protease was determined by incubating the enzyme with various organic solvents at final concentrations of 25.0 % (v/v) including isopropanol, ethanol, methanol, dimethyl ether, diethyl ether, benzene, toluene, chloroform, acetone, butanol, and amyl alcohol at 40 °C for 1 h with shaking. Then, the residual protease activities were measured at standard assay conditions.

Finally, the stability and compatibility of free and immobilized protease in several commercial laundry detergents available in the local market were investigated, including Persil, Ariel, Tide, Bonux, X-TRA, REX, OMO, and Ayam. The enzyme was mixed with an equal volume of each detergent solution with final concentration of 1 % (w/v) (in tap water) and incubated for 24 h at room temperature. The endogenous proteases contained in these detergents were inactivated by pre-incubating the diluted detergents for 10 min in boiling water bath, prior to addition of the NPST-AK15 protease. The enzyme activity measured in the absence of any additives was used as a control.

Kinetic studies

Kinetic studies of free and immobilized NPST-AK15 protease were performed by measuring the enzyme activity at various concentrations of casein ranging from 0.1 to 1.0 % (w/v). The kinetic parameters, including K_m and V_{max} , of free and immobilized protease were estimated using the double reciprocal plot Lineweaver–Burk plot [26]. The value of the turnover number (k_{cat}) was calculated from the equation: $k_{\text{cat}} = V_{\text{max}}/[E]$, where $[E]$ is the

enzyme concentration in the reaction mixture and V_{\max} is the maximal velocity.

Operational stability and reusability

The operational stability and reusability of the immobilized NPST-AK15 protease were evaluated in successive cycles using 2 mL of the standard assay mixture. The reaction mixture containing the immobilized enzyme was incubated in a shaking water bath (120 rpm) at 40 °C for 20 min. At the end of each cycle, immobilized enzyme was separated from the reaction mixture using an external magnetic field, washed with glycine buffer (50 mM, pH 8), to remove any substrate or products remaining with the nanoparticles, and resuspended in a freshly prepared substrate solution to restart a new cycle. The activity was estimated at the end of each cycle as described above, and the residual activity was calculated and expressed relative to the initial immobilized protease activity.

Statistical analysis

The experiments and assays were carried out in triplicate, and the mean values and standard deviation were plotted. Data were analyzed using analysis of variance (ANOVA) by Sigma Stat version 2.03, and statistically significant values (p value >0.05) were noted.

Results and discussion

Synthesis and characterization of RT-MCMSS nanoparticles

Functionalized- and non-functionalized RT-MCMSS nanoparticles were synthesized for immobilization of NPST-AK15 protease by covalent attachment and physical adsorption, respectively. Magnetic nanoparticles (Fe_3O_4) were synthesized by solvothermal reaction, and then the nanoparticles (40–50 nm) were coated with a thin dense silica layer (15 nm), to avoid dissolution of Fe_3O_4 nanoparticle onto the mother system under acidic conditions. Then, mesoporous silica shell (20 nm), in which functional groups can be accommodated for enzyme immobilization, was formed. To impart Fe_3O_4 @meso- SiO_2 core-shell structure more storage capacity for protease immobilization, the rattle-type magnetic core-shell nanoparticles structure was formed through selective etching by controlled dissolution of the middle dense silica layer to form a cavity between Fe_3O_4 @dense- SiO_2 and the outer mesoporous silica shell [20]. Finally, amino- and ethane-functionalized RT-MCMSS nanoparticles were synthesized by post-functionalization approach. TEM images of RT-MCMSS nanoparticles with different functionalization are shown in Fig. 2.

Fig. 2 TEM images of **a** Fe_3O_4 nanoparticles, **b** Fe_3O_4 /dense SiO_2 , **c** Fe_3O_4 @mesoporous SiO_2 and **d** rattle-type Fe_3O_4 @mesoporous SiO_2 core-shell nanoparticles

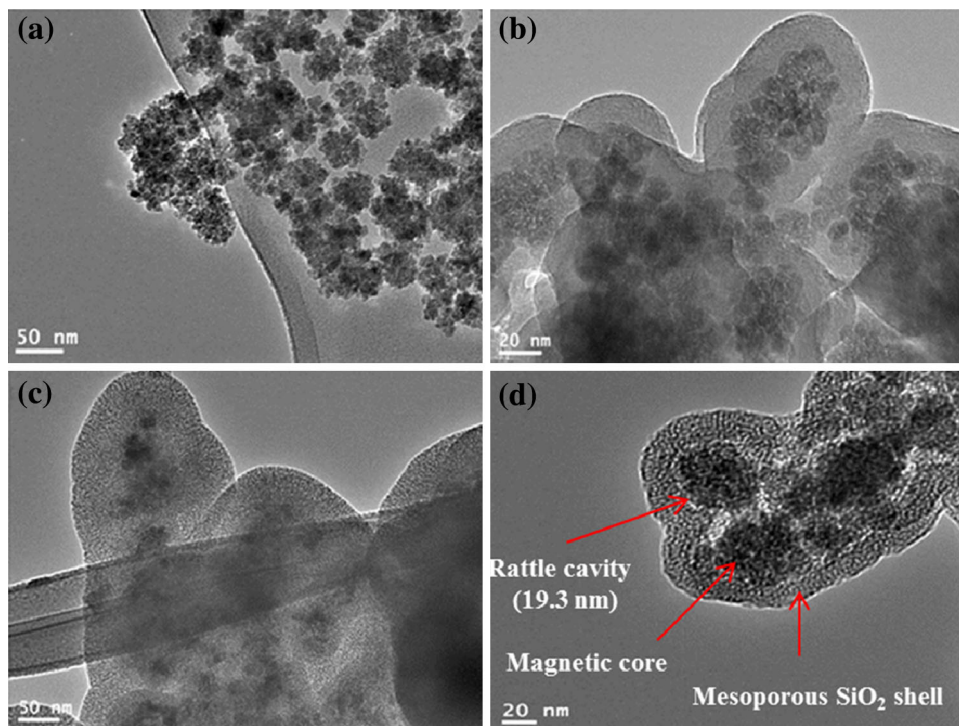


Table 1 Textural properties of rattle-type Fe₃O₄@mesoporous SiO₂ core-shell nanoparticles with different functionalization

Sample code	Total pore volume (V_T) (cc g ⁻¹)	BET surface area (cm ² g ⁻¹)
RT-MCMSS-non	0.322	209.74
RT-MCMSS-NH ₂	0.289	139.61
RT-MCMSS-C ₂ H ₅	0.271	110.35

X-ray diffraction patterns of Fe₃O₄, Fe₃O₄@dense-SiO₂, Fe₃O₄@dense-SiO₂@meso-SiO₂ and rattle-type Fe₃O₄@meso-SiO₂ nanoparticles (Fig. S1) indicated that peaks can be indexed to the spinel magnetite phase and are consistent with the characteristic diffraction peaks of standard Fe₃O₄ (JCPDF card number: 86-1354) [27]. In addition, peak sharpness with no extra peaks indicated the magnetite was formed of well-defined crystallites of high purity. Furthermore, after different functionalization of RT-MCMSS, similar XRD patterns were obtained with no notable change, indicating that the magnetite structure was retained.

The nitrogen adsorption/desorption isotherms (Fig. S2) for the RT-MCMSS nanoparticles samples with different functional groups exhibited the type IV curves, which are characteristic of uniform mesoporous structures that are due to outer mesoporous silica shell [28]. As shown in Table 1, non-functionalized RT-MCMSS showed highest surface area and total pore volume, followed by RT-MCMSS-NH₂, and RT-MCMSS-C₂H₅, respectively. The decrease of BET surface area and total pore volume upon functionalization is most probably due to some blockage of the silica mesopores by functional groups. In addition, the reduction in the surface area and pore volume of ethane-functionalized rattle nanoparticle was slightly higher as compared to particles with amino groups, which can be attributed to higher density of ethane groups as well as to their larger size. On the other hand, pore size distribution also depicts the status of the formed mesopores with and without different functionalities (Fig. S2). Non-functionalized rattle sample show dual mesopores of 3.6 and 19.3 nm for mesoporous channels and rattle cavity, respectively. On the other hand, amino- and ethane-functionalized rattle sample showed dual mesopores at 3.6, 19.3 and 3.6, 16.1 nm, respectively. These results indicate the formation of mesochannels and rattle cavity in case of all three samples. Furthermore, the addition of the functionalization process with amino and ethane groups did not narrow the diameter of mesochannel. However, decrease of the rattle cavity size from 19.3 to 16.1 nm up on functionalization with ethane group might indicate the accumulation of the ethane functional groups within the rattle cavity more than mesochannels.

The magnetic properties of various nanoparticles revealed that no remanence was observed in any sample which indicated their super-paramagnetic character (Fig. S3). The magnetic saturation value for Fe₃O₄ was 81 emu/g, which decreased to 59 and 42 emu/g upon formation of dense silica layer around Fe₃O₄ and rattle-type nanoparticles, respectively. This gradual decrease of magnetization character can be attributed to shielding effect of dense and mesoporous silica layers [29]. However, it had no significant effect on the magnetic separation of the nanoparticles from the bulk solution by the external magnetic field.

FT-IR measurements were performed to confirm different functionality within RT-MCMSS nanoparticles structure (Fig. 3). Non-functionalized rattle structure showed characteristic peak of Fe₃O₄ nanoparticles such as Fe–O at 580 cm⁻¹ together with that of silica, Si–O peak at 1050–1250 cm⁻¹ [30]. On the other hand, RT-MCMSS-NH₂ was elucidated from the existence of N–H peak at 1637 cm⁻¹ [30]. RT-MCMSS-C₂H₅ structure was confirmed by observation of CH₂–CH₂ group that can be seen at 1415 cm⁻¹ together with C–H stretching vibrations peak at 2862 cm⁻¹ indicating the presence of hydrophobic ethane groups within rattle structure [31].

Enzyme immobilization

The specific activity of the purified enzyme was 7285.2 U/mg protein. NPST-AK15 protease was immobilized onto the synthesized RT-MCMSS nanoparticles by two different methods including physical adsorption and covalent attachment. Enzyme immobilization by physical adsorption was performed using three synthesized rattle Fe₃O₄@dense-SiO₂@meso-SiO₂ nanoparticle samples that included RT-MCMSS-non, RT-MCMSS-NH₂, and RT-MCMSS-C₂H₅. For covalent immobilization, the amino-functionalized nanoparticles (RT-MCMSS-NH₂) were first activated by glutaraldehyde as a bifunctional cross linker. The free amino groups lining the mesochannels and rattle cavity of RT-MCMSS-NH₂ nanoparticles react with one of the terminal aldehyde groups of glutaraldehyde molecules to form a Schiff-base and leave the other aldehyde group free that can then be condensed with free amino groups in protease molecules to form a second Schiff-base [32]. The results presented in Table 2 indicated that NPST-AK15 alkaline protease was successfully immobilized on various rattle rattle-type magnetic core@mesoporous shell silica nanoparticles, either by physical adsorption or covalent attachment. However, NPST-AK15 protease immobilization by covalent attachment showed much higher immobilization yield (91.2 %) and loading efficiency (91.4 %) compared to the physical adsorption, which is one of the

Fig. 3 FT-IR spectra of **a** non-functionalized, **b** amino-functionalized and **c** ethane-functionalized rattle Fe_3O_4 @mesoporous SiO_2 core-shell nanoparticles

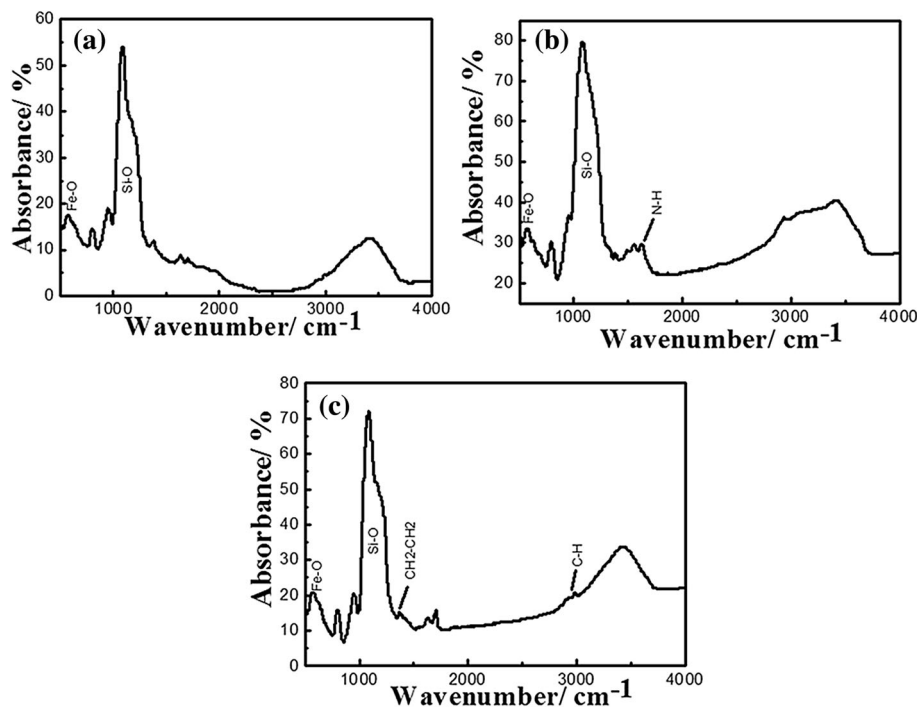


Table 2 Immobilization of NPST-AK15 alkaline protease onto various RT-MCMSS nanoparticles by physical adsorption and covalent attachment

Nanosupport	Immobilization method	Immobilization yield (%)	Activity yield (%)	Loading efficiency (%)
RT-MCMSS-non	Physical adsorption	33.6	31.1	35.8
RT-MCMSS-NH ₂	Physical adsorption	35.2	30.1	28.6
RT-MCMSS-C ₂ H ₅	Physical adsorption	27.5	25	25.9
Activated RT-MCMSS-NH ₂	Covalent attachment	91.2	89.6	91.4

The standard deviations were in the range of 2.1–3.5 %

highest immobilization yield reported for a protease [10]. This is due to the strong covalent bonds formed between the protease molecules and the activated matrix through the coupling agent (glutaraldehyde). On the other hand, the low immobilization yield of the NPST-AK15 protease by physical adsorption suggested low electrostatic/hydrophobic interaction between the enzyme molecules and rattle-type nanoparticles [14]. Thus, the covalent attachment approach was superior for NPST-AK15 protease immobilization onto the activated RT-MCMSS-NH₂ nanoparticles and was used for further studies.

The binding of NPST-AK15 protease to magnetic nanoparticles was confirmed by FT-IR analysis of soluble and immobilized enzymes. The FT-IR spectrum of free protease (Fig. 4a) showed a strong peak at 1550–1650 cm^{-1} which corresponds to the amide I and amide II groups in the protease [9]. The strong broad band that appeared at 3100–3600 cm^{-1} can be attributed to N–H stretching of amide bond present in the enzyme [9]. The

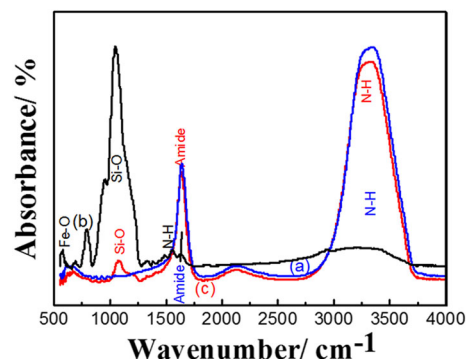


Fig. 4 FTIR spectra of **a** Free NPST-AK15 protease enzyme (blue), **b** amino-functionalized rattle Fe_3O_4 @mesoporous SiO_2 core-shell nanoparticles (black) and **c** NPST-AK15 protease immobilized on amino-functionalized rattle Fe_3O_4 @mesoporous SiO_2 core-shell nanoparticles (red) (color figure online)

immobilization of NPST-AK15 protease on RT-MCMSS-NH₂ nanoparticles was confirmed from the FT-IR spectrum which is displayed in Fig. 4c. The presence of a strong

peak at 1550–1650 cm^{-1} for amide and broad peak at 3100–3600 cm^{-1} for N–H stretching of the protease enzyme was observed together with the main peaks of rattle core–shell nanoparticle as Si–O bond at 1050–1250 cm^{-1} suggested the conjugation of the enzyme with the nanoparticles. Moreover, the slight shift of the Si–O peak to higher wave number could be another evidence for the protease linkage with rattle core–shell nanoparticles.

Loading capacity of RT-MCMSS-NH₂

The loading capacity of activated RT-MCMSS-NH₂ nanoparticles was determined by covalent immobilization of different amounts of NPST-AK15 protease and ranged from 5 to 300 μg protein per mg nanoparticles. The results showed that the amount of loaded protease increased with increasing protein amount giving a maximum of 122.3 μg protein/mg carrier, and plateaued thereafter (Fig. 5). The loading capacity of RT-MCMSS-NH₂ nanoparticles is one of the highest values obtained for a protease immobilization reported, which can be attributed to the availability of high surface area (139.61 $\text{cm}^2 \text{g}^{-1}$) and pore volume of the nanoparticles (0.289 Vt/cc g^{-1}) for the enzyme attachment, and the superior storage capacity of the matrix owing to more nanospaces (19.3 nm) created by formation of rattle structure (creating a cavity between outer mesoporous silica shell and inner silica coated Fe₃O₄ nanocore) [7, 19, 32]. On the other hand, the total activity of the immobilized NPST-AK15 protease increased with increasing the protein concentration up to 114.3 μg per mg nanoparticles. However, further increase in the protein concentration led to a slight decrease in total activity of the immobilized protease (Fig. 5). This is likely due to the steric hindrance of protease molecules within the mesochannels and rattle cavity of RT-MCMSS-NH₂ nanoparticles [25]. Therefore, in all

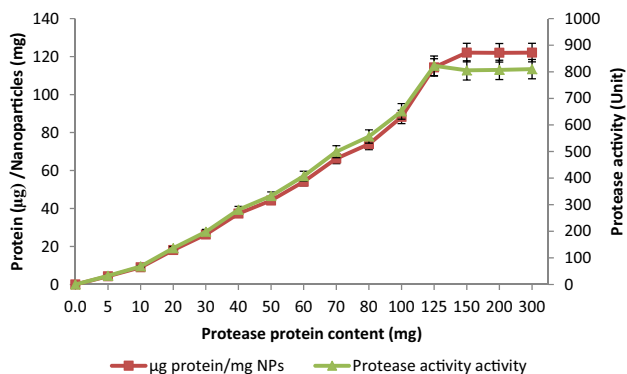


Fig. 5 Loading efficiency of the rattle-type magnetic core/mesoporous shell silica nanoparticles for immobilization of NPST-AK15 protease

subsequent experiments, a protein loading of 114.3 μg protein per mg nanoparticles was employed.

Properties of the immobilized NPST-AK15 protease

Effect of temperature

The influence of temperature on the catalytic activity of free and immobilized NPST-AK15 protease is presented in Fig. 6a. The optimum temperature of free and immobilized enzyme was 60 and 65 $^{\circ}\text{C}$, respectively. In addition, the immobilized enzyme showed higher relative activities than free enzyme, particularly at high temperatures (70–75 $^{\circ}\text{C}$). Observed change in optimum temperature of NPST-AK15 protease activity upon immobilization is consistent with some previous reports [8, 34]. Investigation of the thermostability (irreversible thermal inactivation) of the free and immobilized protease indicated that the soluble enzyme lost about 70 % of its initial activity when incubated at 55 $^{\circ}\text{C}$ for 1 h, whereas under the same conditions, the immobilized enzyme retained 88.3 % of its initial activity (Fig. 6b). Moreover, while the free enzyme almost completely inactivated when treated at 60 $^{\circ}\text{C}$ for 1 and 2 h, the immobilized enzyme retained 66.5 and 39.4 % of its initial activity, respectively. The improved thermostability of the immobilized NPST-AK15 protease is most probably

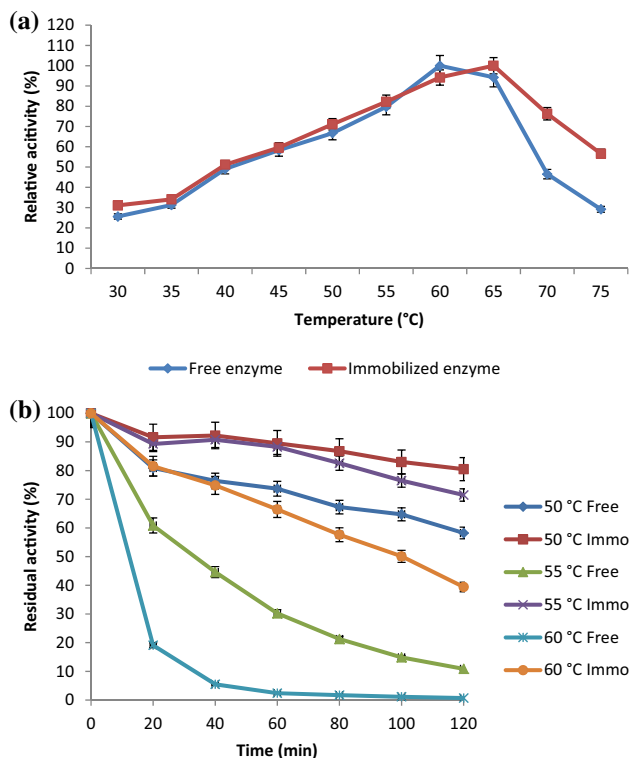


Fig. 6 Effect of temperature on activity (a) and stability (b) of free and immobilized NPST-AK15 alkaline protease

due to multipoint covalent conjugation of enzyme molecules to the support that prevent them from unfolding upon heating [35]. In addition, a vicinal effect induced by the enzyme immobilization in the nanospaces of the mesochannels (3.6 nm) and rattle cavity (19.3 nm) within the RT-MCMSS-NH₂ nanoparticles may favor the rigidification of the enzyme through H-bonds, leading to the improved thermal stability of the immobilized enzyme [24]. Enhancement of thermostability of NPST-AK15 protease upon covalent immobilization onto the RT-MCMSS-NH₂ nanoparticles, suggested that this nanocomposite may be an attractive nanobiocatalyst for industrial applications [12]. Increasing the enzyme thermostability has significant operational advantages, such as higher reaction and diffusion rates, high substrate solubility, and reduced risks from microbial [1].

Effect of pH

The influence of pH on the activity of free and immobilized NPST-AK15 protease revealed that the catalytic activity increased with increasing pH; reaching maximum activity at pH 10.5 and 11.0 for free and immobilized protease, respectively (Fig. 7a). Furthermore, there was a slight increase in the pH stability of the immobilized NPST-AK15 protease in comparison with the free enzyme. The free and immobilized NPST-AK15 protease retained 81 and 86 % of the initial activity after treatment for 3 h at pH 12.0 (data not shown). An increase in the optimum pH was

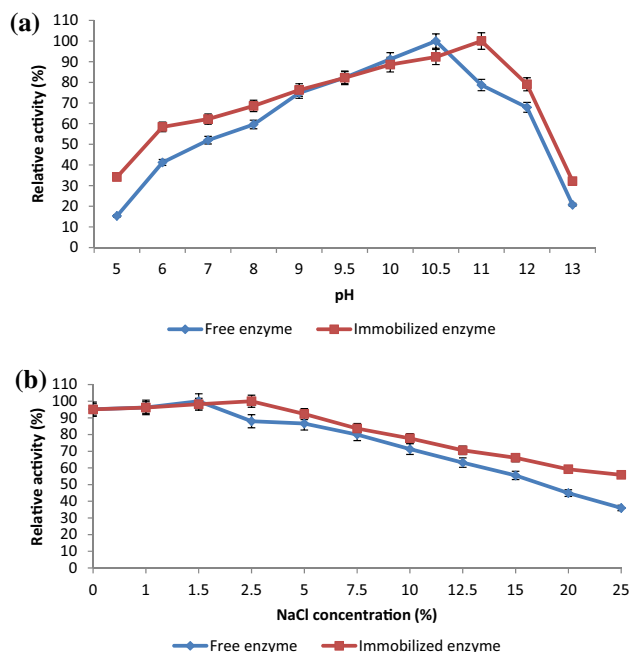


Fig. 7 Effect of pH (a) and salinity (b) on the activity of free and immobilized NPST-AK15 alkaline protease

observed for the immobilized protease [32, 34]. The shift in the optimum pH can be explained by an alteration in the microenvironment of the enzyme due to the immobilization process and interaction between the residual charges on solid support and the protein molecules that may affect active-sites residues [32].

Investigation of the effect of sodium chloride on the activity of free and immobilized NPST-AK15 protease revealed that the enzyme retained activity over a wide range of salt concentrations from 0 to 25 % (w/v), with maximum activity at 1.5 and 2.5 % for free and immobilized enzymes, respectively (Fig. 7b). Moreover, the immobilized enzyme showed higher relative activities compared to the free enzyme particularly at higher NaCl concentrations (10–25 %, w/v). In addition, both free and immobilized enzymes were stable in very high salt concentrations, retaining approximately 65 % of its initial activity at sodium chloride concentrations of 20 % (data not shown). High activity and stability of the NPST-AK15 protease immobilized onto RT-MCMSS-NH₂ nanoparticles suggest its effectiveness as a nanobiocatalyst in applications using ground water under high salt concentrations [36].

Kinetics studies

Kinetics parameters of both free and immobilized NPST-AK15 alkaline protease were estimated using Lineweaver–Burk plot using casein as substrate (Fig. 8; Table 3). The results revealed that K_m value for the immobilized protease is slightly lower (2.0 mg mL^{-1}) than the free enzyme (2.5 mg mL^{-1}), indicating higher affinity of the immobilized protease toward the substrate than the soluble enzyme. This likely due to enzyme expanding within the nanoscale spaces of the mesochannels and rattle cavity of RT-MCMSS-NH₂ nanoparticles resulting in better enzyme orientation, leading to higher affinity of substrate [32, 35], in addition to the high mass transport of reactants and

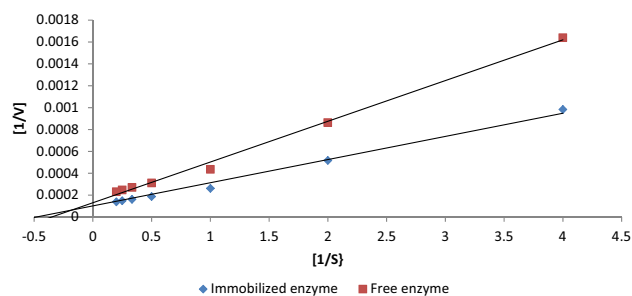


Fig. 8 Estimation of kinetic parameters of the free and immobilized NPST-AK15 protease. The enzyme activity was measured at various casein concentrations (1.0–10.0 mg/mL) at pH 10.5 and 60 °C. The K_m and V_{max} values were determined using linearized Lineweaver–Burk plot

Table 3 Kinetic parameters of free and immobilized NPST-AK15 alkaline protease

Kinetic parameters	Free alkaline protease	Immobilized alkaline protease
K_m (mg mL ⁻¹)	2.5	2.04
V_{max} (μM min ⁻¹ mg ⁻¹)	41.2	55.1
k_{cat} (s ⁻¹)	1187.75	1589.43
k_{cat}/K_m (mM ⁻¹ s ⁻¹)	10,926.8	17,919.2

The standard deviations were in the range of 1.4–3.5 %

products within the matrix which is a characteristic feature of the mesoporous silica-based nanoparticles [12]. Furthermore, the mobility of the nanoparticles themselves via Brownian motion enhances substrate-to-enzyme interactions [11]. Interestingly, the NPST-AK15 immobilized protease showed 1.3-fold higher k_{cat} (enzyme turnover number) and 1.6-fold k_{cat}/K_m (catalytic efficiency) than the soluble enzyme suggesting that the conformational changes of the NPST-AK15 protease due to covalent conjugation within the nanoscale spaces of the mesochannels and rattle cavity of the nanoparticles led to an improvement in enzyme performance. Only few immobilized enzymes showed such enhancement of kinetic parameters of the immobilized enzyme [37].

Effect of surfactants, solvents, and commercial detergents

Since many substrates are not water soluble, the employment of biocatalysts in organic solvents is becoming an important requirement. The use of proteases in organic media has gained much interest in the last decade owing to the potential application of proteases in peptide and ester synthesis under non-aqueous conditions [38]. The effect of various organic solvents on the stability of free and immobilized NPST-AK15 protease revealed 1.2-, 1.3-, 1.4-, and 1.4-fold enhancement in the stability of immobilized protease in ethanol, isopropanol butanol, and amyl alcohol, respectively, relative to free enzyme (Fig. 9a). In addition, its stability in methanol, toluene, and chloroform was increased by about 1.1-fold. The enhancement in stability in organic solvents for NPST-AK15 protease immobilized onto RT-MCSS-NH₂ nanoparticles is most likely due to protection of the native enzyme conformation through the multipoint covalent attachment to the support and entrapment of the protease within mesochannels and rattle cavity of the nanoparticles.

The effect of some surfactants on the stability of free and immobilized NPST-AK15 alkaline protease was investigated. The results illustrated in Fig. 9b indicated that stability of the enzyme in Triton and SDS was significantly enhanced by up to 1.6- and 2.9-fold upon immobilization,

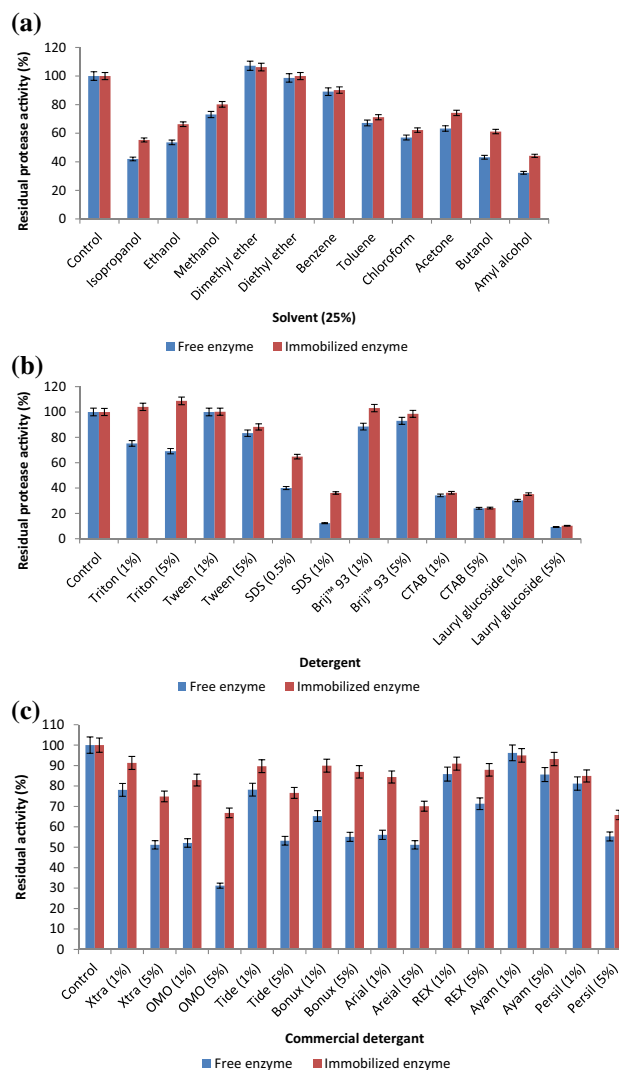


Fig. 9 Effect of organic solvents (a), surfactants (b) and commercial detergents (c) on stability of free and immobilized NPST-AK15 protease stability

respectively. In addition, the stability of immobilized protease in BrijTM 93 and lauryl glucoside was improved by about 1.2-fold. Finally to evaluate the compatibility and feasibility of using NPST-AK15 alkaline protease immobilized onto RT-MCMSS nanoparticles as a laundry detergents additive, its stability toward some commercial laundry detergents was studied. The results presented in Fig. 9c show that the immobilized protease was stable and compatible in most commercial laundry detergents. In addition, the immobilized enzyme exhibited higher stability in OMO, Bonux, Aerial, Xtra and Tide by about 2.1-, 1.6-, 1.5-, 1.5-, and 1.4-fold, respectively, compared to the free protease. The remarkable stability of immobilized protease in various commercial detergents suggests that the nanobiocatalyst is a promising candidate for laundry-cleaning formulations.

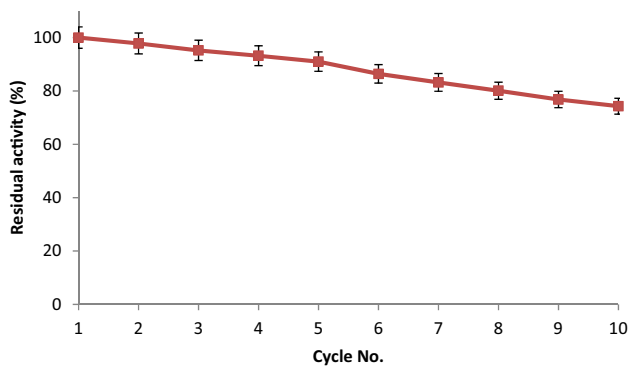


Fig. 10 Reusability of NPST-AK15 protease immobilized within RT-MCMSS nanoparticles

Reusability of immobilized protease

The full industrial application of enzymes is still limited by their high cost in addition to operational stability [1]. Inactivation and enzyme leaching are the most prominent drawbacks for large-scale application of the immobilized enzymes [33]. We have investigated the repeated use of RT-MCMSS-NH₂ immobilized NPST-AK15 protease preparation in several batches of substrate hydrolysis runs at 40 °C. The immobilized protease was separated from the reaction solution after each cycle by applying an external magnetic field. The results (Fig. 10) demonstrated that the immobilized protease could retain up to 91 and 75 % of its initial activity after recycling for five and ten successive reactions, respectively, suggesting a significant operational stability of the developed nanobiocatalyst. The reusability of immobilized protease is very important parameter for cost-effective use of the enzyme either in repeated batch or in continuous processes [1].

Conclusion

Amino-functionalized rattle-type magnetic core@mesoporous shell silica (RT-MCMSS) proved to be an effective nanostructured carrier for NPST-AK15 alkaline protease by covalent immobilization. The superior storage capacity of the matrix owing to more nanospaces created by formation of rattle structure, in addition to high surface area and pore volume of the nanoparticles, led to high immobilization yields and loading efficiency. The NPST-AK15 protease showed significant improvement in activity and stability against temperature, pH and high salt upon immobilization in addition to avoiding activity-stability trade-off. Enzyme immobilization is generally accompanied by a significant reduction in activity due to structural rigidification, however, one of the key findings of this study is that both stability and activity were enhanced in

defiance of activity-stability tradeoff as shown for chemically modified lipase [39]. Interestingly, the immobilized protease exhibited significant enhancement of protease stability in variety of organic solvents, surfactants and commercial laundry detergents. Moreover, the immobilized enzyme exhibited good operational stability and can be recycled multiple times using an external magnetic field. To best of our knowledge this is the first report about immobilization of alkaline protease onto rattle-type magnetic core@mesoporous shell silica nanoparticles. The developed immobilized alkaline protease is a promising nanobiocatalyst for laundry detergents formulation and various bioprocesses for alkaline protease applications.

Acknowledgments This project was funded by the National Plan for Science, Technology and Innovation (MAARIFAH), King Abdulaziz City for Science and Technology, Kingdom of Saudi Arabia, Award Number (12 BIO2899-02).

Compliance with ethical standards

Conflict of interest We have no potential conflict of interest.

References

- Siddiqui KS (2015) Some like it hot, some like it cold: temperature dependent biotechnological applications and improvements in extremophilic enzymes. *Biotechnol Adv* 33:1912–1922
- Raval VH, Pillai S, Rawa CM, Singh SP (2014) Biochemical and structural characterization of a detergent-stable serine alkaline protease from seawater haloalkaliphilic bacteria. *Process Biochem* 49:955–962
- Sathishkumar R, Ananthan G, Arun J (2015) Production, purification and characterization of alkaline protease by ascidian associated *Bacillus subtilis* GACAS8 using agricultural wastes. *Biocatal Agric Biotechnol* 4:214–220
- George N, Chauhan PS, Kumar V, Puri N, Gupta N (2014) Approach to ecofriendly leather: characterization and application of an alkaline protease for chemical free dehairing of skins and hides at pilot scale. *J Clean Prod* 79:249–257
- Ertan H, Cassel C, Verma A, Poljak A, Charlton T, Aldrich-Wright J, Omar SM, Siddiqui KS, Ricardo C (2015) A new broad specificity alkaline metalloprotease from a *Pseudomonas* sp. Isolated from refrigerated milk: role of calcium in improving enzyme productivity. *J Mol Catal B Enzym* 113:1–8
- Haddar A, Agrebi R, Bougatef A, Hmidet N, Sellami-Kamoun A, Nasri M (2009) Two detergent stable alkaline serine-proteases from *Bacillus mojavensis* A21: purification, characterization and potential application as a laundry detergent additive. *Bioresour Technol* 100:3366–3373
- Kamran A, Rehman H, Ul-Qader S, Baloch A, Kamal M (2015) Purification and characterization of thiol dependent, oxidation-stable serine alkaline protease from thermophilic *Bacillus* sp. *J Genet Eng Biotechnol* 13:59–64
- Jin X, Li J, Huang P, Dong X, Guo L, Yang L, Cao Y, Wei F, Zhao Y, Chen H (2010) Immobilized protease on the magnetic nanoparticles used for the hydrolysis of rapeseed meals. *J Magn Mater* 322:2031–2037
- Kumar AG, Swarnalatha S, Kamatchia P, Sekaran G (2009) Immobilization of high catalytic acid protease on functionalized

- mesoporous activated carbon particles. *Biochem Eng J* 43:185–190
10. Ibrahim AS, Al-Salamah AA, El-Toni A, El-Tayeb MA, Elbadawi YB (2014) Cyclodextrin glucanotransferase immobilization onto functionalized magnetic double mesoporous core–shell silica nanoparticles. *Electron J Biotechnol* 17:55–64
 11. Ansari SA, Husain Q (2011) Potential applications of enzymes immobilized on/in nano materials: a review. *Biotechnol Adv* 30:512–523
 12. Lee CH, Lin TS, Mou CY (2009) Mesoporous materials for encapsulating enzymes. *Nano Today* 4:165–179
 13. Ding Sh, Cargill A, Medintz I, Claussen J (2015) Increasing the activity of immobilized enzymes with nanoparticle conjugation. *Curr Opin Biotechnol* 34:242–250
 14. Lei C, Soares TA, Shin Y, Liu J, Ackerman EJ (2008) Enzyme specific activity in functionalized nanoporous supports. *Nanotechnol* 19:125102–125111
 15. Liu J, Qiao SZ, Chen JS, Lou XW, Xing X, Lu GQ (2011) Yolk/shell nanoparticles: new platforms for nanoreactors, drug delivery and lithium-ion batteries. *Chem Commun* 47:12578–12591
 16. Ibrahim AS, Al-Salamah AA, El-Badawi YB, El-Tayeb MA, Antranikian G (2015) Detergent-, solvent- and salt-compatible thermoactive alkaline serine protease from halotolerant alkaliphilic *Bacillus* sp. NPST-AK15: purification and characterization. *Extremophiles* 19(5):961–971
 17. Deng H, Li X, Peng Q, Wang X, Chen J, Li Y (2005) Monodisperse magnetic single-crystal ferrite microspheres. *Angew Chem Int Ed* 44:2782–2785
 18. Deng Y, Qi D, Deng C, Zhang X, Zhao D (2008) Superparamagnetic high-magnetization microspheres with an Fe₃O₄@SiO₂ core and perpendicularly aligned mesoporous SiO₂ shell for removal of microcystins. *J Am Chem Soc* 130:28–29
 19. El-Toni AM, Khan A, Ibrahim AM, Labis PJ, Badr G, Al-Hoshan M, Yin S, Sato T (2012) Synthesis of double mesoporous core–shell silica spheres with tunable core porosity and their drug release and cancer cell apoptosis properties. *J Colloid Interface Sci* 378(1):83–92
 20. Yang J, Shen D, Zhou L, Li W, Li X, Yao C, Wang R, El-Toni AM, Zhang F, Zhao D (2013) Spatially confined fabrication of core–shell gold nanocages@mesoporous silica for near-infrared controlled photothermal drug release. *Chem Mater* 25(15):3030–3037
 21. Yang J, Zhang F, Chen Y, Qian S, Hu P, Li W, Deng Y, Fang Y, Han L, Luqman M, Zhao D (2011) Core–shell Ag@SiO₂@mSiO₂ mesoporous nanocarriers for metal-enhanced fluorescence. *Chem Commun* 47:11618–11620
 22. Shi B, Wang Y, Ren J, Liu X, Zhang Y, Guo Y (2010) Superparamagnetic aminopropyl functionalized silica core–shell microspheres as magnetically separable carriers for immobilization of penicillin G acylase. *J Mol Catal B Enzym* 63:50–56
 23. Ibrahim AS, Al-Salamah AA, El-Toni AM, El-Tayeb MA, Elbadawi YB (2013) Immobilization of cyclodextrin glucanotransferase on aminopropyl-functionalized silica-coated superparamagnetic nanoparticles. *Electron J Biotechnol* 16:1–8
 24. Lowry OH, Rosebrough NJ, Farr AL, Randall J (1951) Protein measurement with the Folin phenol reagent. *J Biol Chem* 193(1):265–275
 25. Song C, Sheng L, Zhang X (2012) Preparation and characterization of a thermostable enzyme (Mn SOD) immobilized on supermagnetic nanoparticles. *Appl Microbiol Biotechnol* 96:123–132
 26. Mathews CK, van Holde KE, van Holde KF (1990) Dynamic of life: catalysis and control of biochemical reactions. Benjamin-Cummings Publishing Company, Subs of Addison Wesley Longman, San Francisco, p 1168. ISBN 978-0805350159
 27. Gong J, Li S, Zhang D, Zhang X, Liu C, Tong Z (2010) High quality self-assembly magnetite (Fe₃O₄) chain like core–shell nanowires with luminescence synthesized by a facile one-pot hydrothermal process. *Chem Commun* 46:3514–3516
 28. Nikolić MP, Giannakopoulos KP, Bokorov M, Srdić VV (2012) Effect of surface functionalization on synthesis of mesoporous silica core/shell particles. *Microporous Mesoporous Mater* 155:8–13
 29. Guo X, Deng Y, Gu D, Che R, Zhao D (2009) Synthesis and microwave absorption of uniform hematite nanoparticles and their core-shell mesoporous silica nanocomposites. *J Mater Chem* 19:6706–6712
 30. Yamaura M, Camilo RL, Sampaio LC, Macedo MA, Nakamura M, Toma HE (2004) Preparation and characterization of (3-aminopropyl)triethoxysilane-coated magnetite nanoparticles. *J Magn Magn Mater* 279:210–217
 31. Zhang L, Liu J, Yang J, Yang Q, Li C (2008) Direct synthesis of highly ordered amine functionalized mesoporous ethane-silicas. *Microporous Mesoporous Mater* 109:172–183
 32. Su R, Shi P, Zhu M, Hong F, Li D (2012) Studies on the properties of graphene oxide–alkaline protease bio-composites. *Bioresour Technol* 115:136–140
 33. Corici L, Frissen A, Zoelen D, Eggen I, Peter F, Davidescu C, Boeriu C (2011) Sol–gel immobilization of Alcalase from *Bacillus licheniformis* for application in the synthesis of C-terminal peptide amides. *J Mol Catal B Enzym* 73:90–9732
 34. Kumari A, Kaur B, Srivastava R, Sangwan R (2015) Isolation and immobilization of alkalineprotease on mesoporous silica and mesoporous ZSM-5 zeolite materials for improved catalytic properties. *Biochem Biophys Rep* 2:108–114
 35. Ranjibakhsh E, Bordbar AK, Abbasi M, Khosropour AR, Shams E (2012) Enhancement of stability and catalytic activity of immobilized lipase on silica-coated modified magnetite nanoparticles. *Chem Eng J* 179:272–276
 36. Jain D, Pancha I, Mishra SK, Shrivastav A, Mishra S (2012) Purification and characterization of haloalkaline thermoactive, solvent stable and SDS-induced protease from *Bacillus* sp.: a potential additive for laundry detergents. *Bioresour Technol* 115:228–236
 37. Mukhopadhyay A, Bhattacharyya T, Dasgupta A, Chakrabarti K (2015) Nanotechnology based activation-immobilization of psychrophilicpectate lyase: a novel approach towards enzyme stabilization and enhanced activity. *J Mol Catal B Enzym* 119:54–63
 38. Jellouli K, Ghorbel-Bellaaj O, Ayed H, Manni L, Agrebi R, Nasri M (2011) Alkaline-protease from *Bacillus licheniformis* MP1: purification, characterization and potential application as a detergents additive and for shrimp waste deproteinization. *Process Biochem* 46:1248–1256
 39. Siddiqui SK, Cavicchioli R (2005) Improved thermal stability and activity in the cold-adapted lipase B from *Candida antarctica* following chemical modification with oxidized polysaccharides. *Extremophiles* 9:471–476